The 9th European Congress on Computational Methods in Applied Sciences and Engineering
ECCOMAS Congress 2024
3 – 7 June 2024, Lisboa, Portugal

BEHAVIOUR OF URM PIERS UNDER HORIZONTAL ACTIONS – COMPARISON OF EXPERIMENTAL AND NUMERICAL RESULTS

I. HAFNER[*], T. KIŠIČEK[*] AND M. GAMS[†]

[*] Faculty of Civil Engineering
University of Zagreb
Fra Andrije Kačića-Miošića 26, Zagreb, Croatia
e-mail: ivan.hafner@grad.unizg.hr, tomislav.kisicek@grad.unizg.hr

[†] Faculty of Civil and Geodetic Engineering
University of Ljubljana
Jamova cesta 2, Ljubljana, Slovenia
email: matija.gams@fgg.uni-lj.si

Key words: Unreinforced masonry piers, Seismic capacity, Numerical modelling, Experimental campaign

1 INTRODUCTION

According to an extensive literature review, masonry is one of the most widely used building materials globally, with approximately 70% of the world's building stock constructed using various types of masonry, as noted by Yavartanoo and Kang [1]. This widespread use is largely due to the simplicity of building with masonry and its high-quality characteristics. Notable advantages of masonry include fire resistance, weather resistance (against heavy storms or high temperatures), and excellent soundproofing capabilities. Despite the long usability period of masonry buildings, there are some drawbacks. Masonry's tendency to absorb moisture can lead to cracking, and its poor tensile strength makes it vulnerable to horizontal forces, especially earthquakes. Barbieri et al. [2] describe seismic vulnerability as the measure of a structure's inadequacy to withstand seismic actions. While earthquakes are not a universal concern, much of Europe and consequently Croatia are known for their high seismicity. In Europe, many buildings with cultural and historical significance, as well as a large portion of residential structures, are built with masonry. Thus, in seismic events, both economic and cultural assets are at risk. These buildings are particularly vulnerable due to their poor tensile strength, often insufficient tying, and the fact that many are constructed before the development of seismic codes. Drougkas et al. [3] confirmed this vulnerability in their study on the seismic behaviour of masonry walls damaged by subsidence.

Given these concerns, a high-level assessment process for existing masonry buildings is essential. Valluzzi [4] emphasized the importance of assessment procedures and their application in historical masonry buildings to develop improvement techniques that enhance safety while meeting preservation and restoration criteria. In the event of an earthquake, comprehensive data collection is crucial. The first step involves a rapid post-earthquake visual assessment using a specific, detailed methodology as described by Stepinac et al. [5]. Following this, various non-destructive methods are employed, including rebound hammers for masonry

and mortar, ground-penetrating radar, ultrasonic pulse velocity tests, impact hammers with accelerometers, thermography cameras, flat jacks, and more, as detailed by Stepinac et al. [6]. These methods are vital for gathering critical information about the building's condition and material characteristics, facilitating more accurate numerical modelling of existing masonry structures. Lulić et al. [7] highlighted the significance of post-earthquake visual assessments and non-destructive surveys in the modelling process. A similar study by Hafner et al. [8] reached the same conclusion, underscoring the need for extensive information collection for proper analysis of an existing building's condition. From everything stated above, proper assessment of unreinforced masonry buildings (URM buildings) and their structural elements is crucial in the post-earthquake renovation process.

The most vulnerable part of an URM building are masonry piers, structural elements placed between windows. The biggest problem is the in-plane shear capacity of these elements. In that regard, URM piers may exhibit three typical in-plane failure modes according to Celano et al. [9] that are categorized as follows:

1) Flexural failure (rocking or toe crushing): failure due to the achievement of the tensile (horizontal cracks – Figure 1a – red lines) or compressive (vertical cracks – Figure 1a – blue lines) strength along the cross end-sections of the wall. The failure mode is typical for slender walls with high compressive stress. In case that the compressive stress is low, a crack opens on the tensile side, but there is no crushing on the compressed side. Such a response is called rocking.

2) Diagonal shear failure: failure related to the achievement of the tensile strength of masonry along the principal direction and characterized by diagonal cracks along the wall that may occur in a stair-step manner through the mortar joints (Figure 1b) or as cracks that propagate in a diagonal straight line (through the bricks as well, Figure 1c).

3) Sliding shear failure: failure occurs along the mortar joints according to horizontal cracks because of the low bond strength at the mortar-masonry interface or due to the reduced values of the compressive stresses acting in the wall (Figure 1d).

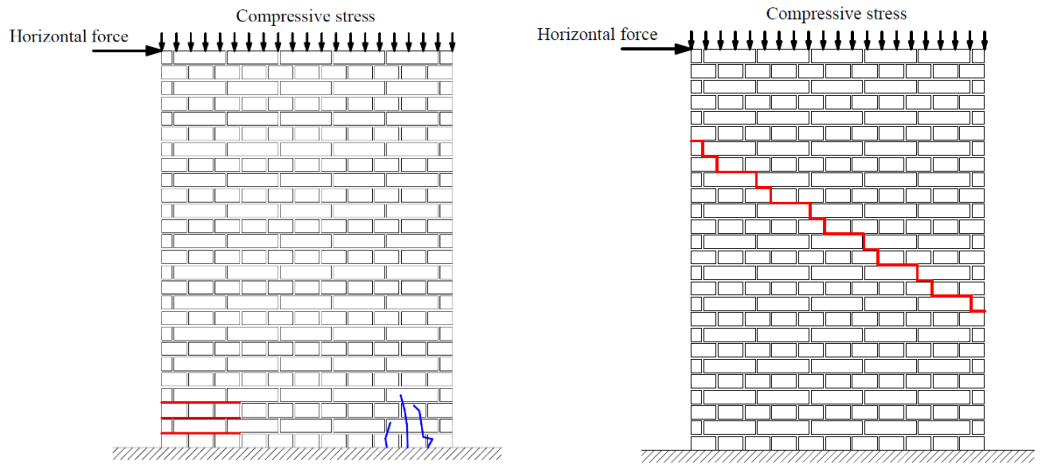

a) b)

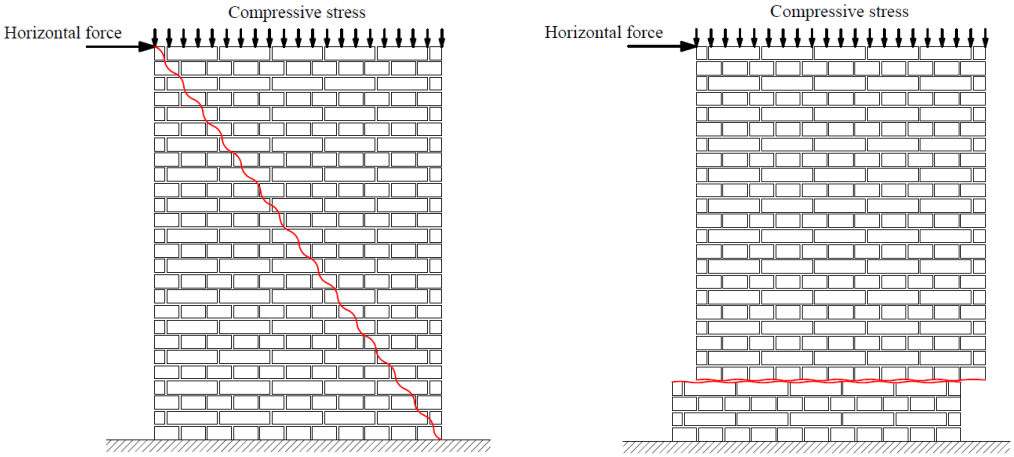

Figure 1: In-plane failure modes of URM walls/piers – a) flexural failure b) diagonal shear failure – stair-step pattern c) diagonal shear failure – diagonal straight crack d) sliding shear failure.

The most common type of masonry pier failure is the diagonal shear failure. Usually, the cracks can be seen only in the vertical and horizontal mortar joints, but cracks through masonry elements are also possible. With this in mind, the behaviour of URM piers under horizontal in-plane shear load and vertical compressive load is examined in the following paragraphs. An experimental and numerical modelling campaign is conducted, and the results are compared with the idea of getting adequate information about the behaviour of URM piers.

2 DEFINITION OF URM PIERS

The dimensions of masonry piers in URM structures vary significantly due to differing architectural styles over the years. To determine the appropriate dimensions for masonry pier samples, a comprehensive review of the literature and existing URM buildings is undertaken. Key factors in defining the pier samples include the desired failure mode and the boundary conditions present in actual masonry piers. The masonry piers with dimensions *l/h/t* = 142/186,5/25 cm are constructed from typical fire clay bricks with dimensions *b/h/l* = 12/6,5/25 cm that are connected by vertical and horizontal mortar layers that are 1 cm thick. The mortar used is lime mortar. The mechanical properties are examined and defined in the following sections. The bricks are placed in two orthogonal directions from one layer to the other. In the first (bottom) layer the bricks are placed perpendicular to the largest surface of the pier. In the following layer the bricks are placed parallel to the largest surface of the pier. This construction pattern continues until the pier is assembled in its full height. The last layer of brick (top layer) matches the bottom layer of the bricks. This type of detailing can be seen in Figure 2. On the top and the bottom of the masonry piers, reinforced concrete beams are placed. The beams with the dimensions *b/h/l* = 45/25/172 cm are used for the purposes of the experimental campaign which will be explained later. The concrete beams are reinforced with 8 ϕ12 longitudinal bars and ϕ8 transversal bars that are placed every 15 cm in the concrete beam. The concrete cover is 2 cm thick.

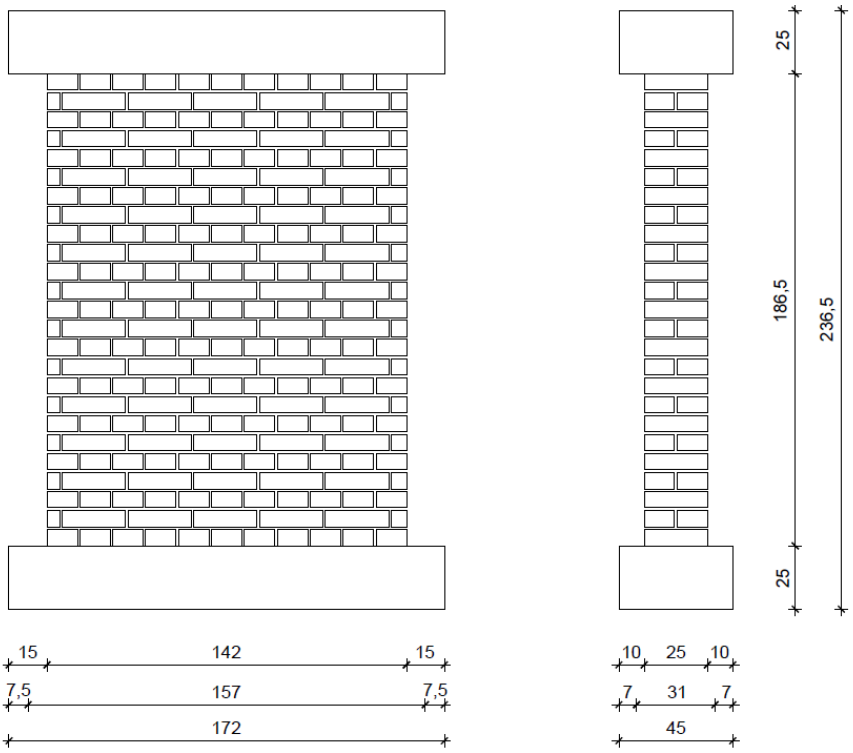

Figure 2: Dimensions of the masonry pier samples

3 THEORETICAL EVALUATION OF URM PIERS

In the theoretical evaluation masonry piers with dimensions *l/h/t* = 142/186,5/25 cm are used as it is defined in the previous section. The theoretical evaluation is based on compression-shear interaction diagrams for URM piers. The values of the vertical compressive force N [kN] are shown on the x-axis and the values of the horizontal in-plane force V [kN] are shown on the y-axis. Seven different failure modes of URM piers with their corresponding shear forces are considered.

The following shear forces are considered:

1) shear force corresponding to flexural failure V_f
2) shear force corresponding to shear sliding (large eccentricity e_n, $f_{vk} < f_{vlt}$) $V_{Rd,1A}$
3) shear force corresponding to shear sliding (large eccentricity e_n, $f_{vk} = f_{vlt}$) $V_{Rd,1B}$
4) shear force corresponding to shear sliding (small eccentricity e_n, $f_{vk} < f_{vlt}$) $V_{Rd,2A}$
5) shear force corresponding to shear sliding (small eccentricity e_n, $f_{vk} = f_{vlt}$) $V_{Rd,2B}$
6) shear force corresponding to diagonal cracking V_d
7) limit value of the shear force corresponding to diagonal cracking $V_{d,\,lim}$

From interaction diagrams, an envelope curve is derived to capture the maximum values of all considered failure modes of URM piers. These interaction diagrams and envelope curves are developed by Jäger and Gams [10]. The envelope curves clearly illustrate how shear resistance and failure mechanisms are affected by material properties, wall geometry, and vertical load. The mechanical properties of the materials used are taken according to literature since no experiments of the mechanical properties are conducted in this phase. These properties

can be seen in Table 1. In this analysis, the contribution of the concrete beams is only accounted for as additional weight on the URM pier. The primary goal of this analysis is to define an appropriate experimental full-scale test setup, including the forces and displacements to be applied in the laboratory.

The interaction diagrams for the URM piers defined by seven different failure modes are shown in Figure 3, while the envelope curve gathered from these failure modes is shown in Figure 4. From the diagram it can be deduced that up until the point marked with A in Figure 4 the URM pier would fail by sliding. After that point and until the value of N = 600 kN the masonry pier exhibits a diagonal shear failure. The maximum vertical compressive force that can be achieved in the laboratory is equal to 300 kN. Since the weight of the pier with reinforced concrete beams is approximately 30 kN, the vertical compressive force of 250 kN is chosen. With the summed value of 280 kN of vertical force, a diagonal shear failure should be achieved. Since the laboratory experiment is conducted by displacement control, the horizontal in-plane force (capacity) V is obtained as a result. The expected value of capacity V when N = 280 kN should be around 150 kN is it can be seen in Figure 4.

Table 1: Properties of masonry units, mortar and masonry piers

Masonry units and mortar						
f_b (N/mm^2)	f_{bt} (N/mm^2)	f_m (N/mm^2)				
40	4,0	5				
Masonry piers						
f_k (N/mm^2)	$\mu=tan(\phi)$	f_{vk0} (N/mm^2)	f_{vlt} (N/mm^2)	f_{tk} (N/mm^2)	h_0 (cm)	γ_m
11,79	0,5	0,2	2,6	0,133	93,25	1,0

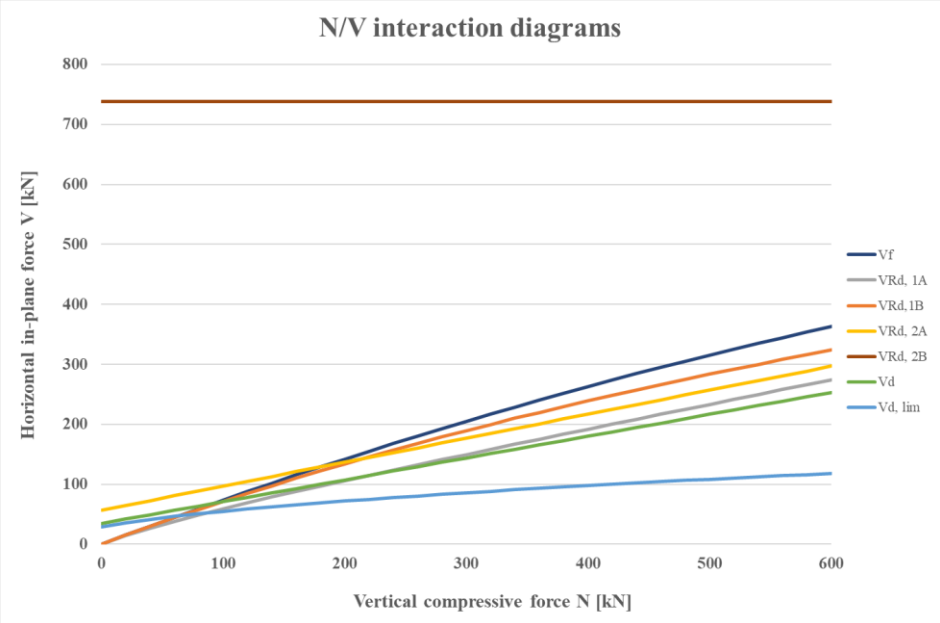

Figure 3: Interaction diagrams *N/V* for seven different failure modes

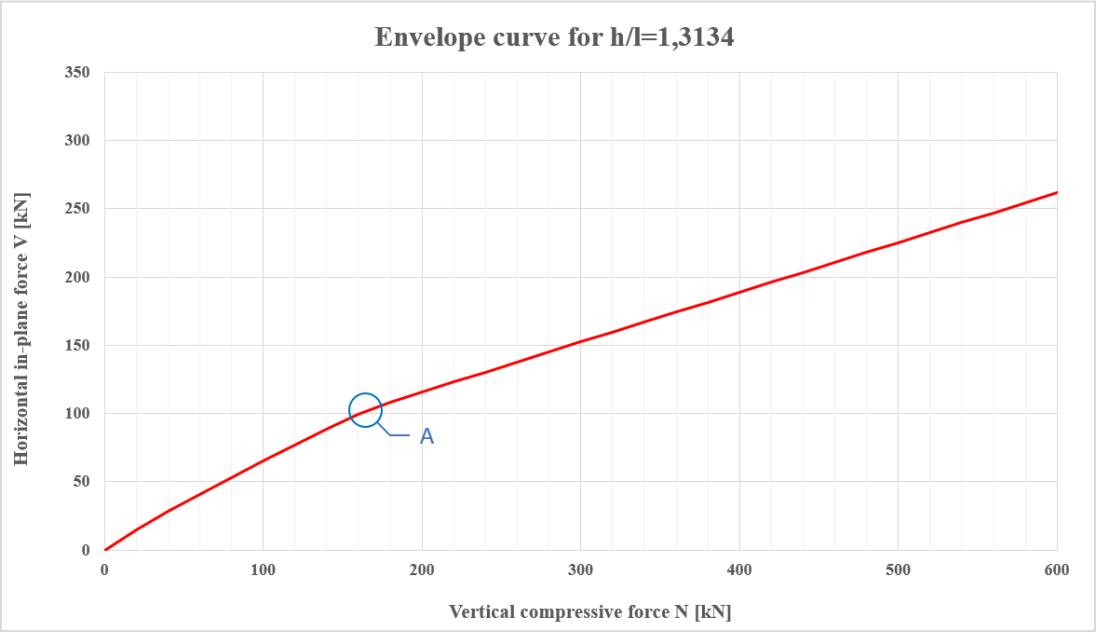

Figure 4: Envelope curve for the analysed URM pier

4 EXPERIMENTAL CAMPAIGN

In the theoretical evaluation of URM piers, the boundary conditions and the vertical compressive force that are going to be used in the experiment are defined. The experimental campaign is divided into two phases. In the first phase, the testing of mechanical properties of materials is conducted. The following mechanical properties are gathered: compressive strength of concrete f_{cm}, compressive strength of masonry units f_{avg}, compressive strength of hardened mortar f_m and the initial shear strength of masonry f_{vk0i}. The results for these mechanical properties are shown in Table 2. The concrete used is denominated with concrete grade C30/37.

Table 2: Mechanical properties of tested materials

f_{cm} [N/mm^2]	f_{avg} [N/mm^2]	f_m [N/mm^2]	f_{vk0i} [N/mm^2]
38,87	32,19	6,12	0,23

In the second phase, the URM piers in full scale are tested. The testing procedure is defined as the quasi-static cyclic displacement-controlled testing procedure. The testing of masonry piers was conducted at the structural testing laboratory at the Faculty of Civil Engineering and Architecture, University of Osijek, Croatia. The schematic display of the test setup is shown in Figure 5.

During construction of URM piers, reinforced concrete beams were installed at both the top and bottom of the pier. The top beam's function is to evenly distribute vertical loads and transfer horizontal forces from the hydraulic jacks. Vertical loading at the top is applied using two hydraulic jacks, each with a capacity of 250 kN. These jacks are supported by a rigid steel reference frame, anchored to a sturdy reactive base and a rigid vertical reactive wall. To ensure smooth horizontal movement and prevent shear deformations due to friction during horizontal

load application, a roller support with a teflon coating and steel rollers is placed between the reinforced concrete beam and the steel plates beneath the hydraulic jacks. The bottom reinforced concrete beam's role is to securely connect and firmly fix the masonry pier to the laboratory floor. This setup, along with the applied vertical forces, prevents any potential overturning of the pier.

The cyclic testing of the shear capacity is conducted in two steps for all three URM piers. First, a gradual vertical force, F_v, is applied until reaching a total value of 250 kN. Two jacks are used each applying a vertical force equal to 125 kN (marked YS 50/100 in **Error! Reference source not found.** 5). The valves on the jacks are closed when the designed compressive stress is achieved. The compressive stress is taken as σ_v = 0,7 MPa, which may be slightly higher than the usual vertical load for a constructed building but is chosen with the specific goal of achieving diagonal shear failure. In the second step, two horizontal jacks are used. The horizontal jack on the left (marked YCH 33/150 in Figure 5) has a maximum displacement range of 150 mm. The horizontal jack on the right (marked YCH 33/250 in Figure 5) has a maximum displacement range of 250 mm. Both horizontal jacks have a force capacity of 335 kN. The quasi-static cyclic testing protocol replicated the seismic effects by the slow application of cyclic displacements. The loading history consisted of stepwise increasing deformation amplitudes. In a complete cycle the target displacement was imposed in the positive and negative loading direction, returning to the original position of the pier. The first step was 1 mm in both directions. In each next step the displacement is increased 1 mm in comparison to the previous step.

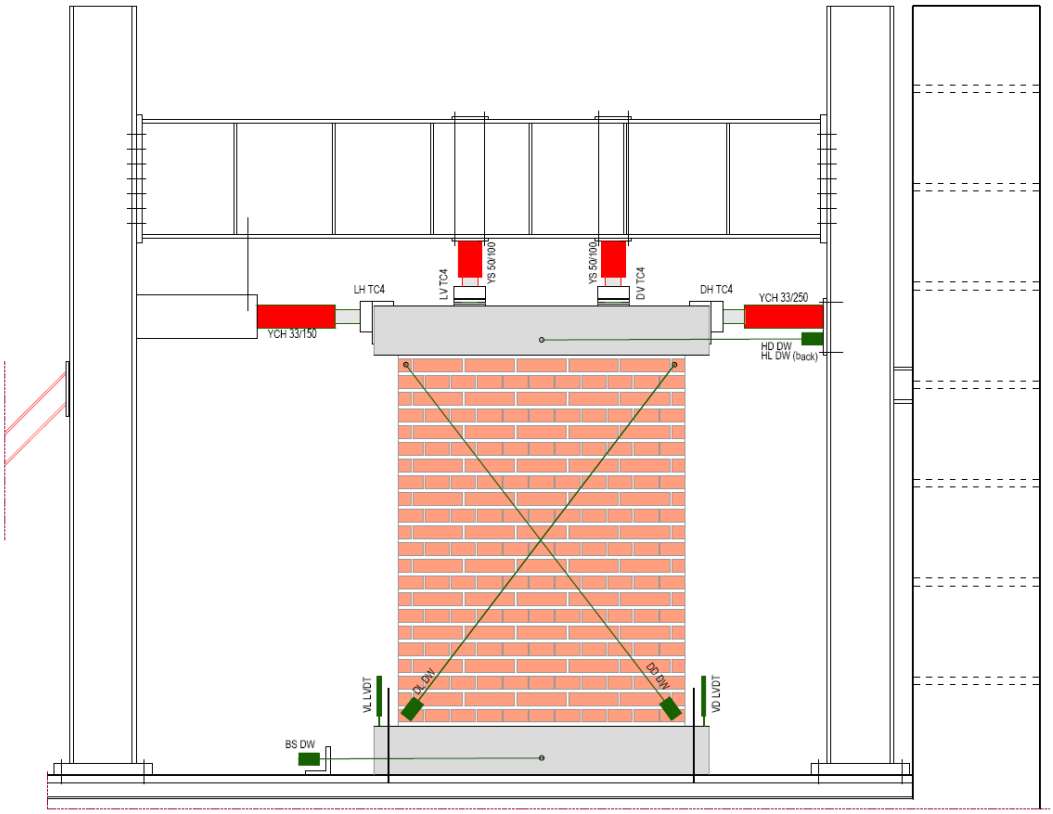

Figure 5: Schematic display of the experimental setup

The results for all three piers are graphically and numerically presented. The graphical representation of results is shown in the form of hysteresis curves (experimental response curves) and resistance envelope curves that are derived from them. The resistance envelope curves are formed by connecting the peak points in the loading cycles under increasing deformations. In these diagrams, on the horizontal axis the horizontal displacement of the pier is shown in millimetres (mm). On the vertical axis the horizontal in-plane force is shown in kilonewtons (kN). The most important values of each curve are shown in tables. The hysteresis and envelope curves for URM 1, URM 2 and URM 3 piers are shown in Figures 6. The most important results that were gathered from these curves are shown in Table 3. It is obvious that the results vary from one URM pier to the other which is attributed to their heterogenic nature. The comparisons are made in the final chapter. The cracking patterns for URM 1, URM 2 and URM 3 piers can be seen in Figure 7 respectively. The diagonal shear cracking pattern and failure are observed in all three cases which is satisfactory and in accordance with the goals of this research.

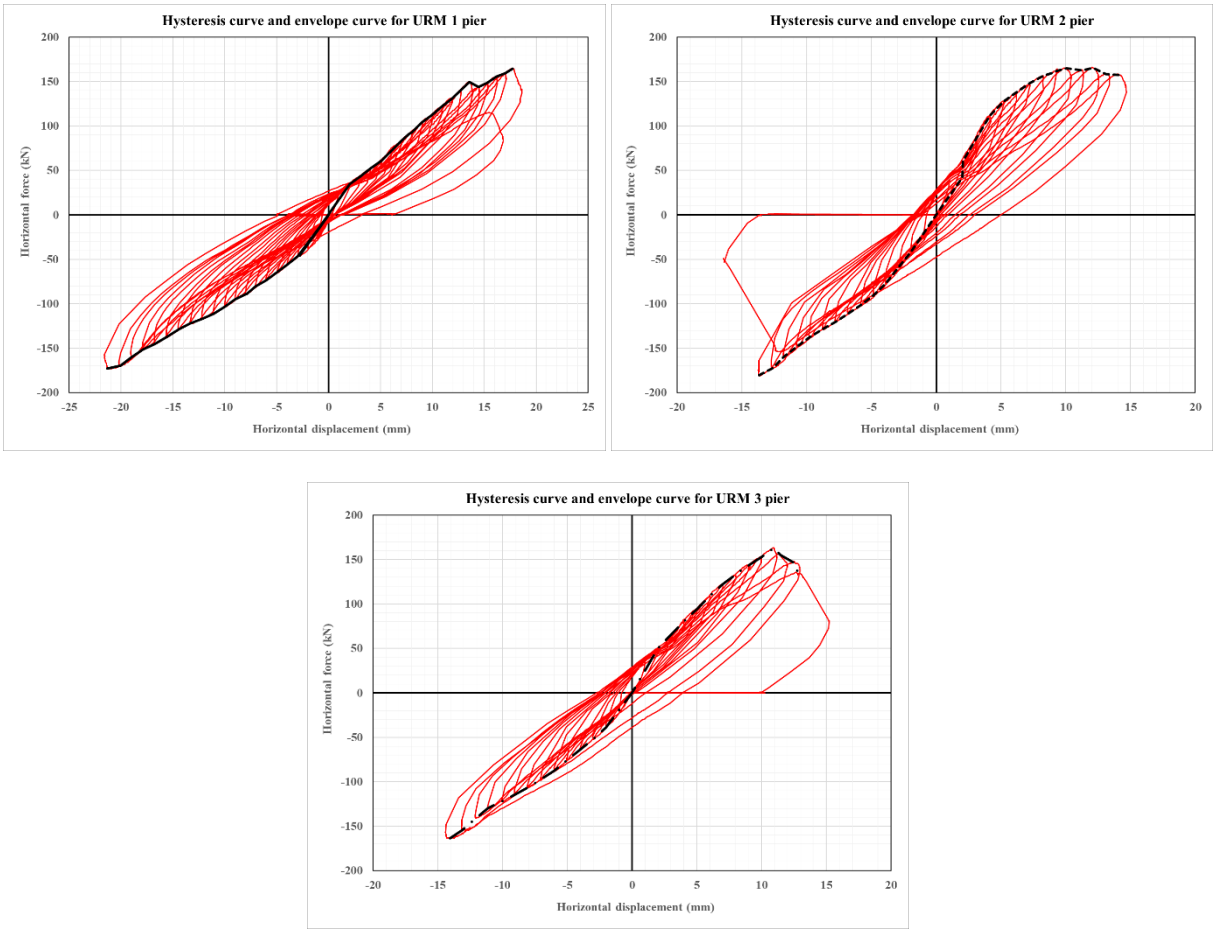

Figure 6: Hysteresis curves and envelope curves for URM 1, URM 2 and URM 3 pier

Table 3: Results of the experimental campaign for URM piers

Value	URM 1	URM 2	URM 3	mean
Maximum horizontal force – positive direction [kN]	148,24	164,34	147,65	153,39
Maximum displacement – positive direction [mm]	17,71	14,10	10,95	14,25
Displacement at yielding point – positive direction [mm]	13,46	9,38	8,31	10,38
Ductility – positive direction	1,32	1,50	1,32	1,38
Maximum horizontal force – negative direction [kN]	167,71	167,06	146,57	160,45
Maximum displacement – negative direction [mm]	21,32	13,68	14,06	16,35
Displacement at yielding point – negative direction [mm]	19,03	11,88	11,61	14,17
Ductility – negative direction	1,12	1,15	1,21	1,16

Figure 7: Cracking patterns of URM 1, URM 2 and URM 3 piers

5 NUMERICAL MODELING

In this research the DIANA FEA 10.4 software is used. Numerous research on this software indicates it is a powerful tool for the numerical modelling of masonry [11]. In this research the micro-modelling approach is chosen. The main advantages of such a micro modelling approach are the most accurate description of the masonry texture, detailed characterization of mechanical properties and explicit crack patterns [12]. The bricks are

modelled as elastic blocks linked together by mortar joint elements. The mortar layers are defined as zero-thickness interface elements between blocks. The reinforced concrete beams at the top and the bottom of the URM pier are defined as one element each. The mechanical properties are shown in Tables 4 and 5. The boundary conditions and loads were applied in the same manner as in the experiment. The URM pier and the resulting cracking pattern of the URM pier are shown in Figure 8. The pushover curve is shown in Figure 9 in red. From Figure 9 it can be obtained that the maximum horizontal force in both directions is equal to 140 kN. The maximum displacement is equal to 11,50 mm, while the displacement at yielding point is equal to 7,85 mm. From these two values, the ductility is calculated with the value of 1,47.

Table 4: Linear elastic properties of concrete and masonry

Element	E **(N/mm^2)**	υ	**Mass density (kg/m^3)**
Concrete beams	33000	0,2	2500
Masonry bricks	12957	0,2	1500

Table 5: Mechanical properties of mortar joints

Normal stiffness k_n (N/mm^3)	**Shear stiffness k_s (N/mm^3)**	**Tensile strength f_t (N/mm^2)**
390	156	0,15
Fracture energy G_f^I (N/mm)	**Cohesion c (N/mm^2)**	**Friction angle (rad)**
0,003	0,23	0,75
Dilatancy angle (rad)	**Residual friction angle (rad)**	**Confining normal stress (N/mm^2)**
0	0,75	-0,7
Exponential degradation coefficient (mm)	**Fracture energy G_f^{II} (N/mm)**	**Compressive strength f_k (N/mm^2)**
5	0,023	11
Factor C_s	**Compressive fracture energy (N/mm^2)**	**Equivalent plastic relative displacement (mm)**
9	26	50

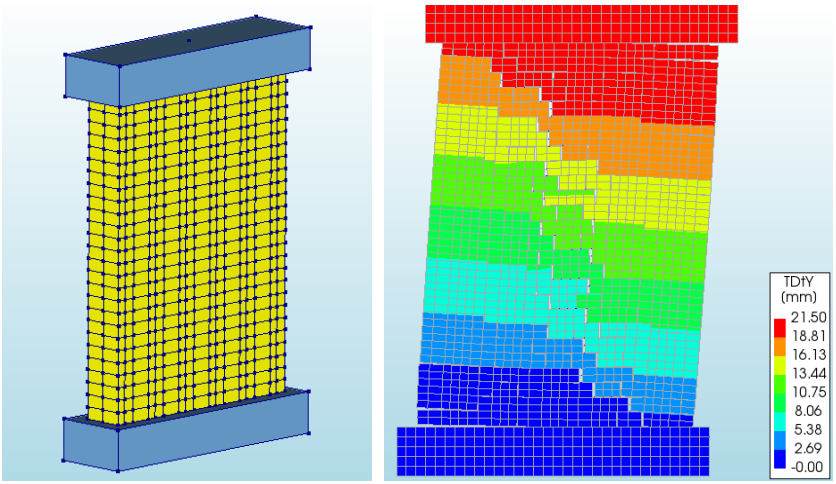

Figure 8: URM pier in DIANA FEA 10.4 software and the cracking pattern of the URM pier

6 COMPARISONS AND CONCLUSIONS

In this section comparisons are drawn between the theoretical, experimental and numerical results. From Figure 9 it can be observed that the numerical model yielded similar results to the experimental campaign. The maximum displacement is smaller than in the experiment due to the conservative nature of the software. On the other hand, from the results given in Table 6 the ductility is very similar for the experimental and numerical modelling campaigns, especially in the positive direction. The maximum horizontal forces are very similar in both positive and negative direction when the experimental and numerical results are compared. Yet again, the numerical model's conservative nature led to smaller values. From Table 6 it can also be concluded that the theoretical preliminary analysis that is conducted in section 3 gives adequate results for URM piers. Finally, it can be concluded that the theoretical evaluation given in seismic provisions and the numerical micro modelling approach can and should be used in the evaluation of URM piers in old masonry buildings.

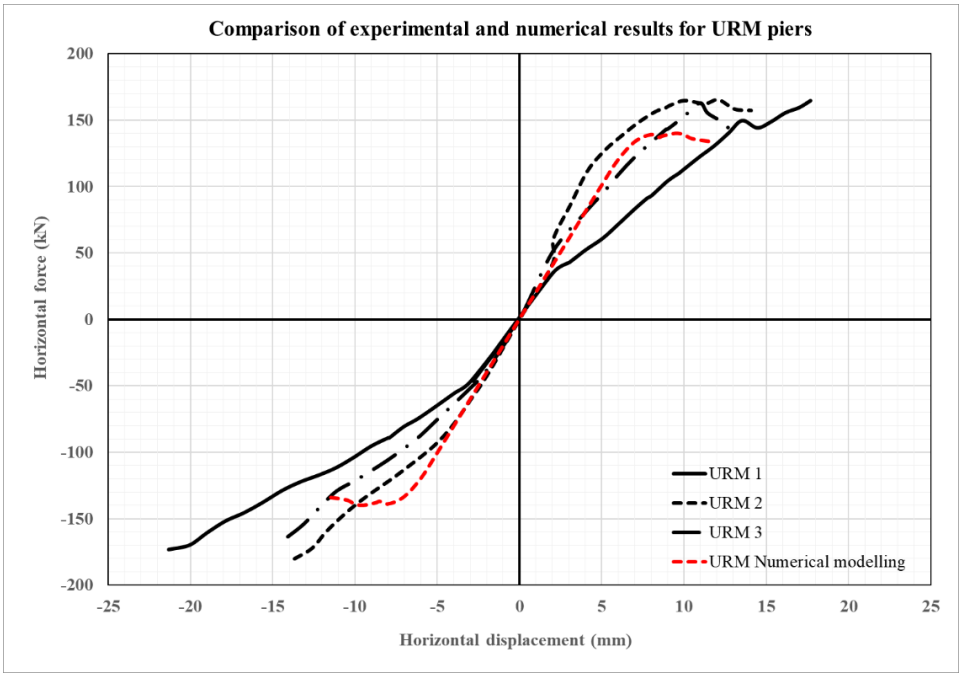

Figure 9: Comparison of experimental and numerical results

Table 6: Theoretical, experimental, and numerical results for URM piers

Value	Theoretical results	Experimental results (mean)	Numerical results
Maximum horizontal force – positive direction [kN]	149,00	153,39	140,00
Maximum displacement – positive direction [mm]	-	14,25	11,50
Ductility – positive direction	-	1,38	1,47
Maximum horizontal force – negative direction [kN]	149,00	160,45	140,00
Maximum displacement – negative direction [mm]	-	16,35	11,50
Ductility – negative direction	-	1,16	1,47

REFERENCES

[1] Yavartanoo, F., Kang, T.H.K.: Retrofitting of unreinforced masonry structures and considerations for heritage-sensitive constructions, *Journal of Building Engineering*, 49

(2022) December 2021, p. 103993.
[2] Barbieri, G., Biolzi, L., Bocciarelli, M., Fregonese, L., Frigeri, A.: Assessing the seismic vulnerability of a historical building, *Engineering Structures*, 57 (2013), pp. 523–535.
[3] Drougkas, A., Licciardello, L., Rots, J.G., Esposito, R.: In-plane seismic behaviour of retrofitted masonry walls subjected to subsidence-induced damage, *Engineering Structures*, 223 (2020) July, p. 111192.
[4] Valluzzi, M.R.: On the vulnerability of historical masonry structures: analysis and mitigation, *Materials and Structures/Materiaux et Constructions*, 40 (2007) 7
[5] Stepinac, M. *et al.*: Damage classification of residential buildings in historical downtown after the ML5.5 earthquake in Zagreb, Croatia in 2020, *International Journal of Disaster Risk Reduction*, 56 (2021) January.
[6] Stepinac, M., Kisicek, T., Renić, T., Hafner, I., Bedon, C.: Methods for the assessment of critical properties in existing masonry structures under seismic loads-the ARES project, *Applied Sciences (Switzerland)*, 10 (2020) 5.
[7] Lulić, L., Ožić, K., Kišiček, T., Hafner, I., Stepinac, M.: Post-earthquake damage assessment-case study of the educational building after the zagreb earthquake, *Sustainability (Switzerland)*, 13 (2021) 11.
[8] Hafner, I., Lazarević, D., Kišiček, T., Stepinac, M.: Post-Earthquake Assessment of a Historical Masonry Building after the Zagreb Earthquake–Case Study, *Buildings*, 12 (2022) 3.
[9] Celano, T., Argiento, L.U., Ceroni, F., Casapulla, C.: Literature review of the in-plane behavior of masonry walls: Theoretical vs. experimental results, *Materials*, 14 (2021).
[10] Jäger, A., Gams, M.: Practical design of masonry subjected to horizontal loads based on Eurocode 6 shear model, *Brick and Block Masonry: Trends, Innovations and Challenges - Proceedings of the 16th International Brick and Block Masonry Conference, IBMAC 2016*, (2016), pp. 689–694.
[11] Aşıkoğlu, A., Vasconcelos, G., Lourenço, P.B., Pantò, B.: Pushover analysis of unreinforced irregular masonry buildings: Lessons from different modeling approaches, *Engineering Structures*, 218 (2020) March.
[12] D'Altri, A.M. *et al.*: D'Altri, A.M. *et al.*: , A review of numerical models for masonry structures, (2019). Elsevier Ltd, 2019, 2019.